Supplementary Data

Supplementary Methods:

Reagents. Recombinant murine M-CSF was obtained from R&D Systems (Minneapolis, MN). Glutathione S-transferase (GST)-RANKL was expressed in our laboratory as described[13]. The source of antibodies and reagents is as follows: c-fos (#2250; 1:1000), Phospho-AKT (Thr 308) (#4056; 1:1000), phosphor-ERK (44/42) (#5726; 1:1000), integrin β3 (#4702; 1:1000), AKT (#2920; 1:1000), phosphor-P38 (#9216; 1:1000), phosphor-IκBα (#9246; 1:1000), IκBα (#4812; 1:1000), EZH2 (#5246; 1:2000), (Cell Signaling); NFATc1 (#sc17834; 1:200), EED (#sc28701; 1:200) (Santa Cruz); beta-actin (#A5316; 1:5000) (Sigma), JMJD3 (#ab 38113; 1:1000), H3K4me3 (#ab 8580; 1:2000) for immunoblots and 5μg antibody for ChIP, H3K27me3 (#ab6002; 1:2000) for immunoblots and 5μg antibody for ChIP (Abcam), Donkey Alexa Fluor 680 anti-rabbit (#A10043:10,000), Alexa Fluor 680 anti-mouse (#A10038:10,000),(ThermoFisher-Scientific), Donkey IRDye 800 CW anti-rabbit (926-32213; 1:10,000) anti-mouse (925-32212; 1:10,000) (Licor). All other chemicals were obtained from Sigma.

Histology and histomorphometry. The tibiae and femur of 13-week old-male mice were fixed with 10% neutral buffered formalin, followed by decalcification in 14% EDTA for 10 days, paraffin embedding, and TRAP staining. Images were collected using the NanoZoomer slide scanner, Alafi Neuroimaging Laboratory. We analyzed one slide per mouse. To quantitate the TRAP positive cells and determine how much of their surface area covered the bone (i.e. OcS/BS) we used the BioQuant OsteoII software (BioQuant Image Analysis Corporation, Nashville, TN). We carried out these measurements by defining a region of interest (ROI) for total tissue volume (TV; 1.5mm below the growth plate and kept same for all femurs analyzed) and bone volume (BV). We then chose a diagonal line type tool to define the bone surface (BS); osteoclast surface (Oc.S) and osteoblast surface (Ob. S). TRAP positive osteoclasts were measured using the number tool on BioQuant software. Osteoblasts were identified morphologically (cuboidal, on bone) on the same sections as the OCs were enumerated. Primary Indices were calculated from these: BV/TV; OcN/BS; ObN/BS. All measurements were done in a blinded fashion.

Microcomputed tomography (μCT). Micro-computed tomography (μCT) was done on femurs of 13-week-old male mice. Bones were fixed in 10% neutral buffered formalin and then embedded in 2% agarose gel. The trabecular volume of the distal femoral metaphysis was measured using a Scanco μCT40 scanner (Scanco Medical AG, Bassersdorf, Switzerland), calibrated using a hydroxyapatite phantom. A threshold of 250 was used for evaluation for all male scans and a threshold of 212 was used for evaluation for all female scans. 50 slices were analyzed, starting with the first slice in which condyles and primary spongiosa were no longer visible. Trabecular bone was contoured to exclude the cortical bone, allowing cancellous bone volume/tissue volume (BV/TV) and bone mineral density (BMD) to be determined. vBMD was measured as mean values of everything within volume of interest (mixture of bone and background). Since scan was calibrated for bone, therefore, the mean value was represented in units of Hydroxyapatite density [mg HA/ccm]

Serum Trap5B, CTX and P1NP measurements: Serum TRAP5B, CTX and P1NP levels were measured by ELISA (Biomedical Technologies Inc.).

FACS Analysis: Whole bone marrow mononucleated cells were obtained using the spin-flushing method followed by red cell lysis, and cells were counted using a hemocytometer. To gain a comprehensive view of osteoclast development, bone marrow cells (approximately 20 x 10^6/animal) were stained with fluorophore-conjugated antibodies including ant-CD34 FITC(eBiosciences; clone RAM34,1:40), anti-CD265 (RANK)-PE(Biolegend; clone R12-31, 1:200), anti-Ly-6A/E (Sca1) PerCP/Cy5.5 (Biolegend; clone D7; 1:200), anti-CD115 PE Dazzle 594 (Biolegend; clone AFS98, 1:200), anti-CD11b PE/Cy7 (Biolegend; clone M1/70, 1:200), anti-CD11c e660 (eBioscience; clone N418, 1:200), anti-CD117 (c-kit) APC e780 (eBioscience; 2B8, 1:200), anti-CD16/32 (FCγ) BV421 (eBioscience; clone 2.4G2, 1:200), eBioscience Flexible Viability Dye e506 (1:1000) and analyzed on Cytek upgraded 3-laser-BD FACScan cytometer by flow cytometry. LSK HSCs were defined as cells lacking the lineage markers CD2, CD3e, Ter119, B220, and Gr1, but which were Sca^+ and $c\text{-}kit^+$. Common Myeloid Progenitor (CMP) cells were defined as $Lineage^-$ $ckit^{Hi}$ $CD34^+$ $Fc\gamma^-$. Granulocyte/Macrophage Progenitor (GMP) cells were defined as $Lineage^-$ $c\text{-}kit^{Hi}$ $CD34^+$ $Fc\gamma^+$. Megakaryocyte/Erythroid Progenitor (MEP) cells were defined as $Lineage^-$ $c\text{-}kit^{Hi}$ $CD34^-$ $Fc\gamma^-$. Osteoclast progenitors were defined as $Lineage^-$ $CD11b^{lo}$ $c\text{-}kit^+$ $CD115^+$ $RANK^+$ cells. To evaluate for possible

hematopoietic defects, bone marrow cells were isolated from one femur from n=5 ASXL1$^{flox/flox}$ female mice and n=5 ASXL1^{cKO} female mice using the spin-flushing method. Cells were resuspended 1 mL of Wash Media (high glucose DMEM containing 5% heat-inactivated FBS, 1X penicillin/streptomycin, and 1X L-glutamine) and passed through a 100 μm nylon mesh. The mesh was washed in 10 mL Wash Media, and centrifuged at 500 x *g* for 5 min at 4 °C. The cell pellets were resuspended in 1.0 mL sterile PBS, and 0.250 mL (one-quarter of the isolated cells) were stained with the viability dye ZombieUV (1:600 in PBS, BioLegend). Cells were centrifuged as above and resuspended in an antibody cocktail containing rat anti-mouse CD45-BUV395 (BD Horizon; clone 30-F11; 1:200), rat anti-mouse TER-119-BV510 (BioLegend; clone TER-119; 1:300), rat anti-mouse/human CD11b-BV650 (BioLegend; clone M1/70; 1:400), rat anti-mouse CD8α-BV711 (BioLegend; clone 53-6.7; 1:300), rat anti-mouse CD19-BV785 (BioLegend; clone 6D5; 1:300), rat anti-mouse F4/80-APC (BioLegend; clone BM8; 1:300), rat anti-mouse CD4-Alexa Fluor 700 (BioLegend; clone RM4-5; 1:300), rat anti-mouse Ly6G-APC/Cy7 (BioLegend; clone 1A8; 1:200), rat anti-mouse SiglecF-PE (BD Pharmingen; clone E50-2440; 1:400), rat anti-mouse Ly6C-FITC (BioLegend; clone HK1.4; 1:300), and hamster anti-mouse CD3ε-PE-CF594 (BD Horizon; clone 145-2C11; 1:300) in Brilliant Stain Buffer (BD Biosciences) containing 10 μg/mL Fc Block (purified unconjugated rat anti-mouse CD16/32; clone 2.4G2; BD Pharmingen). Cells were incubated in the staining cocktail on ice for 30 min. Stained cells were washed three times in 200 μL FACS Buffer (PBS containing 2.5% heat-inactivated FBS and 2.5 mM EDTA) before data acquisition on a five-laser BD X20 flow cytometer. A gating strategy shown in Supplemental Figure 5A was used to define TER-119^{+} CD45^{-} red blood cells, CD3^{+} T cells, CD3^{+} CD4^{+} T cells, CD3^{+} CD8^{+} T cells, CD4^{-} CD8^{-} T cells, CD19^{+} B cells, SiglecF^{+} SSC^{hi} eosinophils, Ly6G^{+} CD11b^{+} neutrophils, Ly6C^{hi} monocytes, Ly6C^{lo} monocytes, and F4/80^{+} CD11b$^{-/lo}$ macrophages. Cells were counted using CountBright Absolute Counting Beads (Invitrogen) for flow cytometry according to manufacturer's instructions, and for each cell type the bead-corrected cell counts were multiplied by 4 to calculate total numbers of each cell type per femur. Cell frequencies were defined as percent of all cells (for red blood cells) or as percent of CD45^{+} cells (for all immune cell populations).

Medium CTx-1 assay: Macrophages were cultured on bone with 100 ng/ml RANKL and 1/50 volume CMG14-12 mouse M-CSF-producing cell line supernatant for 6 days. The medium (α-10) was changed 1 day before

harvesting. Medium CTx-1 concentration was determined using the CrossLaps for Culture ELISA kit (Nordic Bioscience Diagnosis A/S). Serum osteocalcin measurements: Serum osteocalcin levels were measured by ELISA (Biomedical Technologies Inc.).

RNA Extraction and quantitative qPCR. RNA from cultured cells was isolated and purified using the RNeasy RNA purification kit (Qiagen); RLT lysis buffer was supplemented with β-mercaptoethanol (1%). Purified RNA was treated with DNase I (Invitrogen) before reverse transcription. cDNA was synthesized from RNA (1 μg) using iScript™ cDNA Reverse Transcription kit (Bio-Rad) per manufacturer's instructions. Real-time PCR was performed using the SYBR Green Master Mix kit and gene specific primers. Quantitative PCR was performed on ABI PRISM 7500 sequence detection system (Applied Biosystems, Foster City, CA). All reactions were performed in triplicates and relative mRNA levels were calculated by the comparative threshold cycle method using cyclophilin as an internal control.

Immunoblot. Cultured cells were washed twice with ice-cold PBS and lysed in radioimmune precipitation assay (RIPA) buffer containing 20 mm Tris-HCl, pH 7.5, 150 mm NaCl, 1 mm EDTA, 1 mm EGTA, 1% Triton X-100, 2.5 mm sodium pyrophosphate, 1 mm β-glycerophosphate, 1 mm Na3VO4, 1 mm NaF, and 1× protease inhibitor mixture (Roche Applied Science). After incubation on ice for 10 min, cell lysates were clarified by centrifugation at 15,000 rpm for 10 min. Forty micrograms of total lysates were subjected to 8–12% sodium dodecyl sulfate polyacrylamide gel electrophoresis and transferred onto PVDF membranes. Filters were blocked in 0.1% casein in PBS for 1 h and incubated with primary antibodies at 4 °C overnight followed by probing with fluorescence-labeled secondary antibodies (Jackson ImmunoResearch Laboratories). Proteins were detected with the Odyssey Infrared Imaging System (LI-COR Biosciences).

UCSC Genome browser URL:

goo.gl/vnWo1i

Supplementary Tables

Supplementary Table 1: Motif enrichment analysis in ASXL1cKO osteoclast with loss in H3K27me3

Rank	P-value	log P-pvalue	% of Targets	% of Background	STD(Bg STD)	Best Match/Details
1	1e-71	-1.641e+02	2.90%	0.00%	51.1bp (15.1bp)	Nkx2.1(Homeobox)/LungAC-Nkx2.1-ChIP-Seq(GSE43252)/Homer(0.591)
2	1e-64	-1.482e+02	2.40%	0.00%	54.6bp (0.0bp)	E2F7(E2F)/Hela-E2F7-ChIP-Seq(GSE32673)/Homer(0.670)
3	1e-64	-1.482e+02	2.40%	0.00%	51.9bp (0.0bp)	PB0148.1_Mtf1_2/Jaspar(0.677)
4	1e-57	-1.316e+02	2.40%	0.01%	60.3bp (72.3bp)	PB0146.1_Mafk_2/Jaspar(0.633)
5	1e-44	-1.035e+02	2.50%	0.02%	51.7bp (44.1bp)	MA0152.1_NFATC2/Jaspar(0.592)
6	1e-28	-6.664e+01	1.20%	0.00%	54.1bp (46.2bp)	ETS(ETS)/Promoter/Homer(0.600)

Supplementary Table 2: Motif Enrichment Analysis in ASXL1cKO osteoclast with H3K4me3

Rank	P-value	log P-pvalue	% of Targets	% of Background	STD(Bg STD)	Best Match/Details
1	1e-64	-1.479e+02	2.40%	0.00%	54.6bp (0.0bp)	E2F7(E2F)/Hela-E2F7-ChIP-Seq(GSE32673)/Homer(0.671)
2	1e-52	-1.215e+02	2.40%	0.01%	56.5bp (32.7bp)	PH0065.1_Hoxc10/Jaspar(0.601)
3	1e-52	-1.204e+02	2.50%	0.01%	51.5bp (58.1bp)	MA0152.1_NFATC2/Jaspar(0.621)
4	1e-48	-1.122e+02	2.10%	0.01%	49.7bp (32.4bp)	Six1(Homeobox)/Myoblast-Six1-ChIP-Chip(GSE20150)/Homer(0.729)
5	1e-35	-8.159e+01	1.60%	0.00%	65.8bp (70.8bp)	PB0090.1_Zbtb12_1/Jaspar(0.586)
6	1e-28	-6.646e+01	1.20%	0.00%	54.1bp (0.0bp)	PH0171.1_Nkx2-1/Jaspar(0.768)

Supplementary Figures

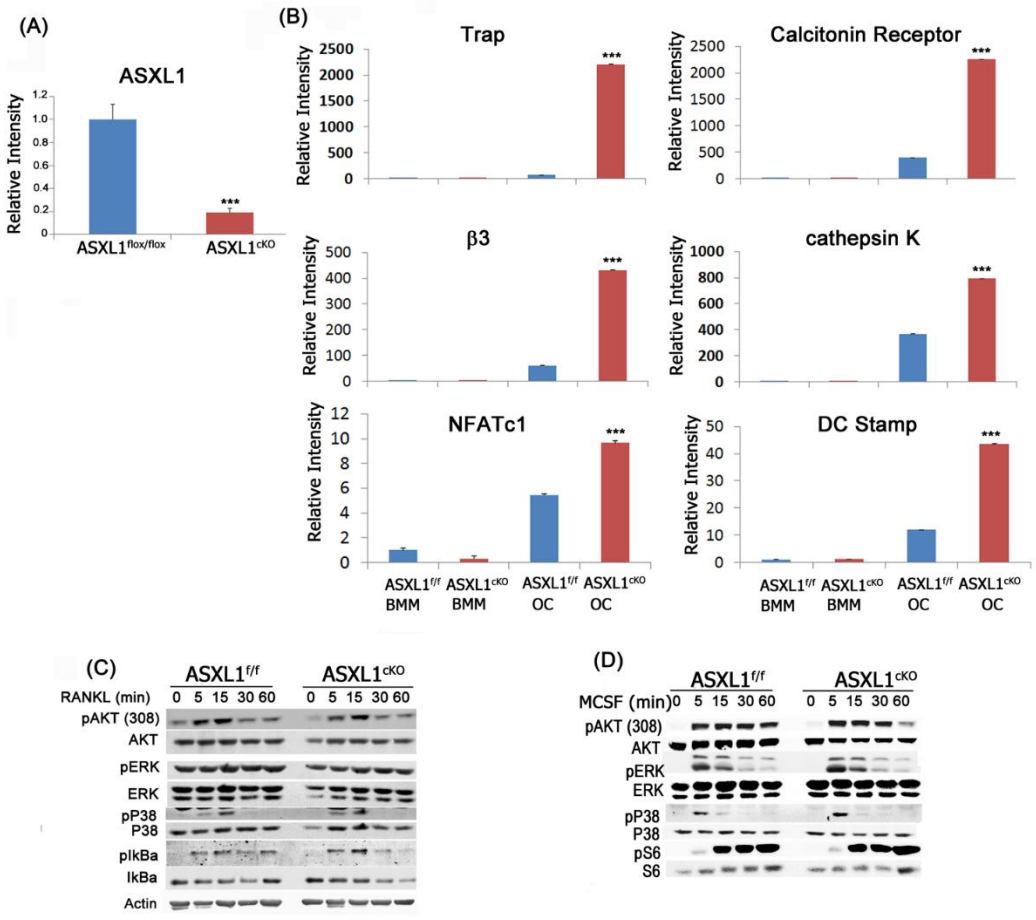

Supplemental Figure 1. Effect of ASXL1 deletion on RANKL and MCSF signaling: (A) ASXl1$^{flox/flox}$ and ASXL1^{cKO} BMMs were exposed to M-CSF and RANKL for 2 days. ASXL1 mRNA expression in ASXl1$^{flox/flox}$ and ASXL1^{cKO} BMMs as determined by qPCR. **(B)** ASXl1$^{flox/flox}$ and ASXL1^{cKO} BMMs cultured in M-CSF and RANKL (50ng/ml) for 2 days. Osteoclast differentiation marker mRNAs were determined by qPCR. For figure A and B, unpaired nonparametric *t*-test was used for statistical analysis. Error bars represent + SD; ***p<0.001. **(C)** Cytokine/serum starved control and ASXL1^{cKO} BMMs were exposed to RANKL (100ng/ml) with time. Cytoplasmic osteoclastogenic signaling molecule activation was determined by immunoblot. β-actin serves as cell lysate loading control. **(D)** Cytokine/serum starved WT and ASXL1^{cKO} BMMs were exposed to M-CSF (100ng/ml) with time. Cytoplasmic osteoclastogenic signaling molecule activation was determined by immunoblot. n=3 independent experiments. BMM: Bone marrow macrophages; OC: osteoclasts

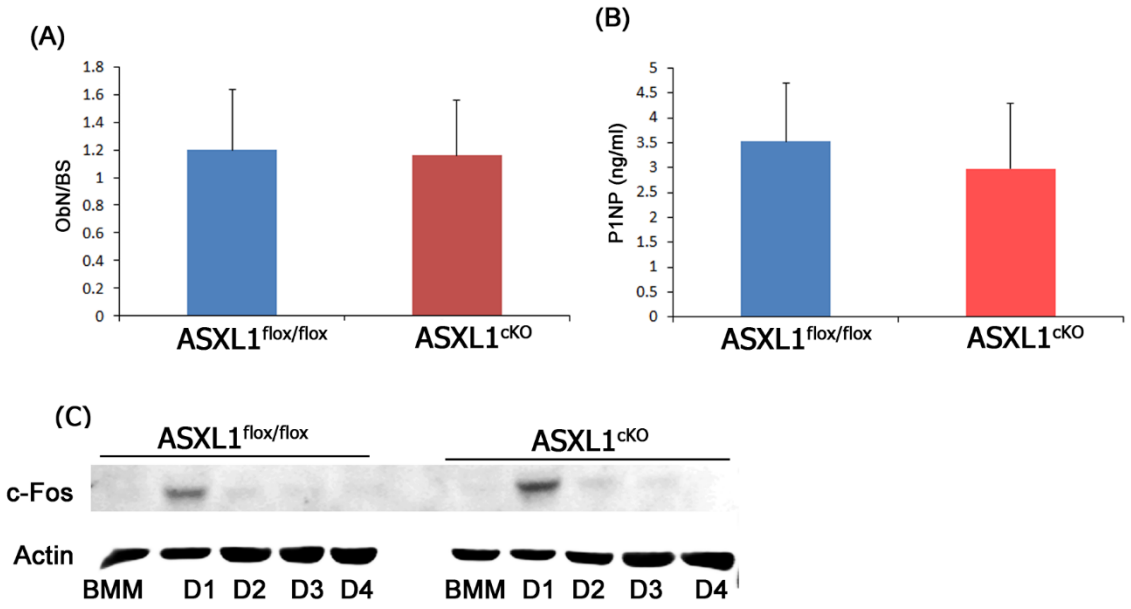

Supplemental Figure 2. ASXL1^{cKO} osteoclast formation is not mediated by c-Fos (A) ASXL1$^{flox/flox}$ and ASXL1^{cKO} femurs of 13-week-old male mice were analyzed for osteoblast number (ObN) per mm bone surface (BS) histomorphometrically (n=5 in each group) **(B)** Serum P1NP of 12-week-old male ASXL1$^{flox/flox}$ and ASXL1^{cKO} mice (n=8 in each group). **(C)** ASXL1$^{flox/flox}$ and ASXL1^{cKO} BMMs were exposed to M-CSF and RANKL for 4 days. c-Fos mRNA abundance was temporally determined by immunoblot. Unpaired nonparametric *t*- test was used for statistical analysis. Error bars represent + SD; ns: no significance.

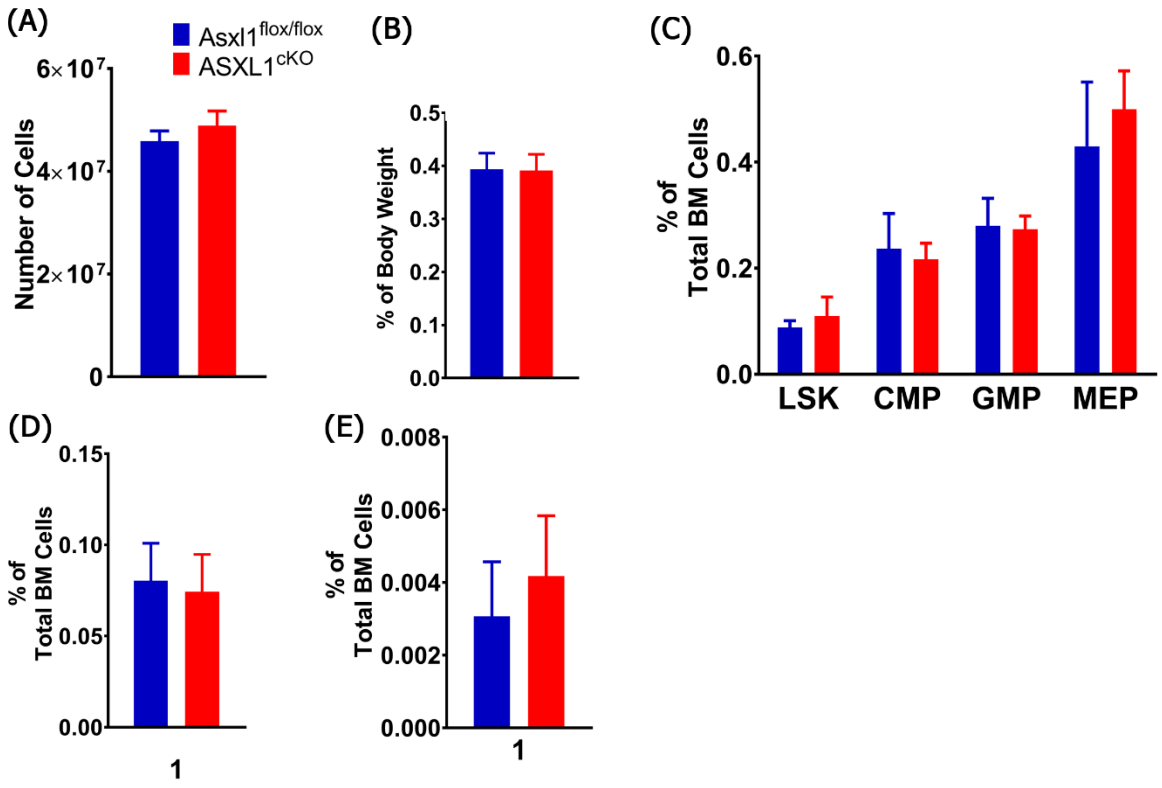

Supplemental Figure 3. Normal hematopoiesis and osteoclast progenitor profile in ASXL1^{cKO} mice. (A) Total mononuclear cell abundance in marrow (BM cellularity) **(B)** and spleen weight normalized to the body weight (splenomegaly index) of 12-week-old male mice **(C)** Marrow myeloid progenitor profile including LSK, CMP, GMP and MEP **(D and E)** Committed marrow residing osteoclast progenitor profile, **(D)** CD11b^{lo}, c-fms^{+}, RANK^{-} **(E)** CD11b^{lo}, c-fms^{+}, RANK^{+}. (n=3 in each group). For figure A, B, D and E, unpaired nonparametric *t*- test was used for statistical analysis. Error bars represent + SD; for figure C, two-way ANOVA was used. No statistical differences were observed.

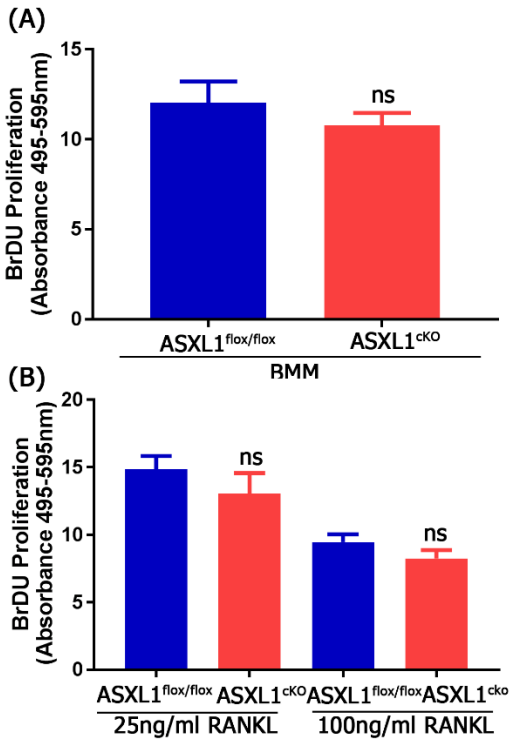

Supplementary Figure 4. BrdU incorporation in BMM and preosteoclasts. Bone marrow macrophages from 6-week-old female ASXL1$^{flox/flox}$ and ASXL1^{cKO} mice were cultured in presence of **(A)** M-CSF or **(B)** RANKL (25 and 100 ng/ml) for 3 days. BrdU was added in the last 3 hrs. of culture. BrdU assay was performed per manufacturer's protocol. ANOVA was used for multiple comparisons. ns: non-significant (n=2 independent experiments)

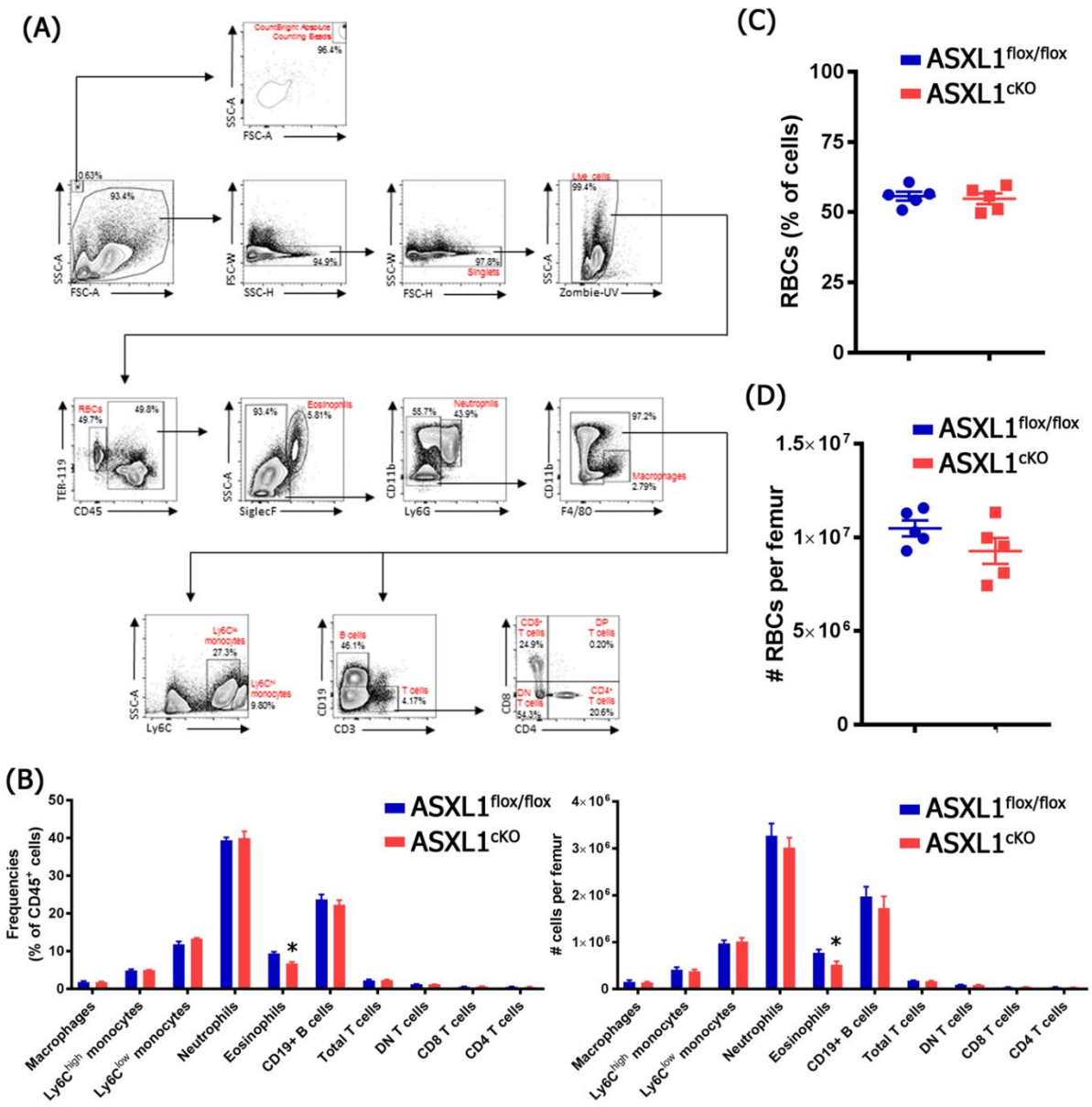

Supplementary Figure 5. Immunophenotypical characterization of bone marrow cells (A) Gating Strategy **(B)** Frequencies and total cell number of each population as indicated in bone marrow of ≤12 weeks age old female mice. **(C and D)** Erythrocyte frequencies and numbers in the bone marrow of ASXL1$^{flox/flox}$ and ASXL1^{cKO} mice. n=5 mice, Two-way ANOVA was used for Fig B and unpaired non- parametric *t*- test was used for figure C and D. No significant difference was observed except for eosinophils ($P < 0.05$ for both left and right panel).

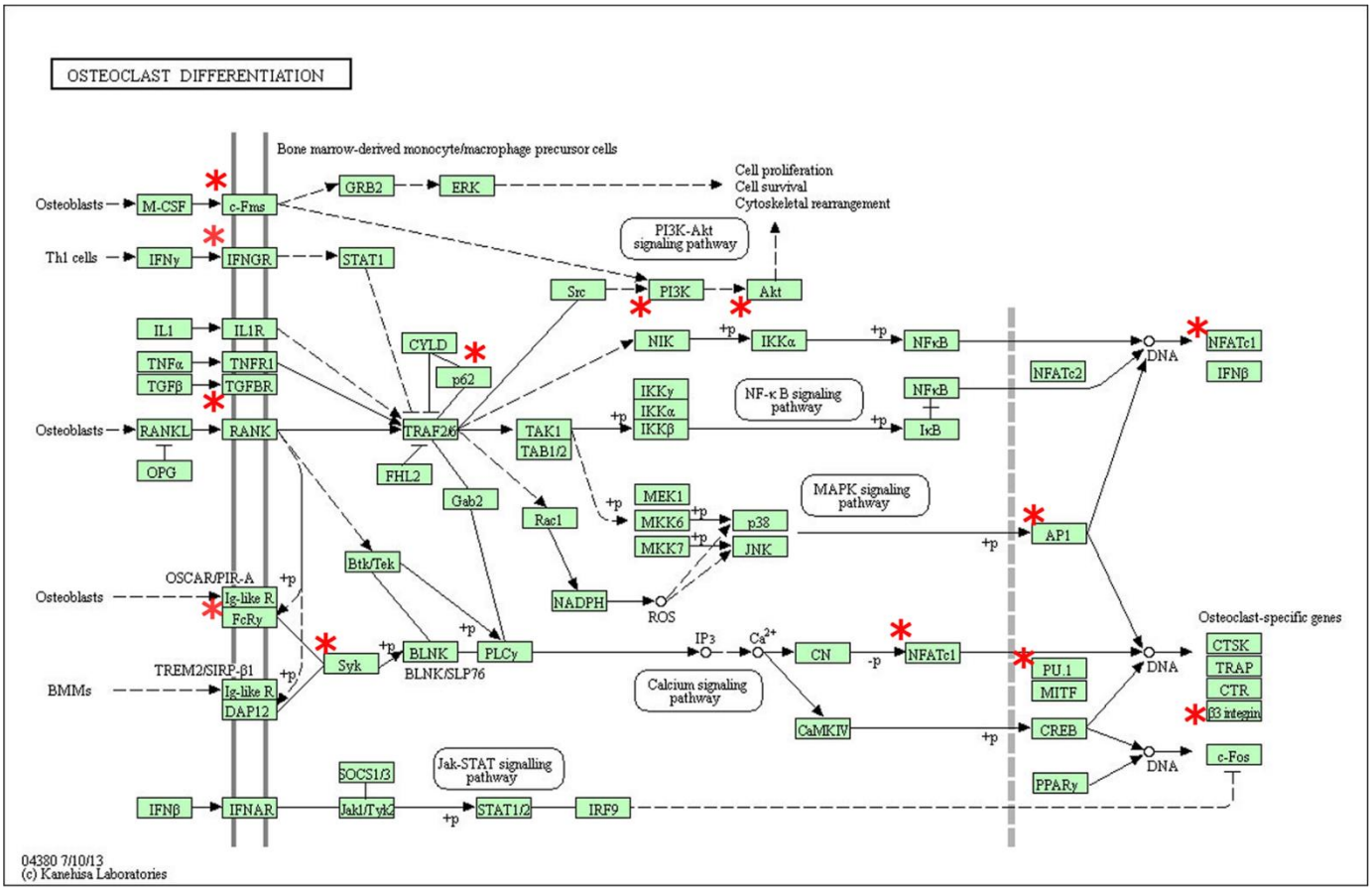

Supplemental Figure 6. ChIP seq analysis: KEGG pathway analysis showing enrichment of osteoclast differentiation pathway. Green boxes represent genes involved in osteoclast differentiation. * represents significant changes between control and KO groups.

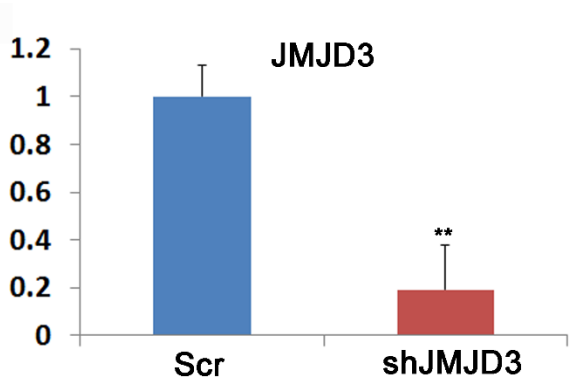

Supplemental Figure 7. JMJD3 knockdown efficiency: (A) ASXL1^{cKO} BMMs, transduced with scrambled or shRNA for JMJD3, were exposed to M-CSF and RANKL (25ng/ml) for 3 days. JMJD3 mRNA abundance was determined by qPCR. Unpaired non- parametric *t*- test was used. ** $p < 0.01$